Proceedings of the Canadian Society for Mechanical Engineering International Congress
32nd Annual Conference of the Computational Fluid Dynamics Society of Canada
Canadian Society of Rheology Symposium
CSME/CFDSC/CSR 2025
May 25–28, 2025, Montréal, Québec, Canada

NUMBER

Conjugate Heat Transfer and Freezing of Impinging Droplets on Coated Steel Substrates

Sahar Goudarzi[1], Yuri S Muzychka[1], Greg F Naterer[2],

[1]Faculty of Engineering and Applied Science, Memorial University of Newfoundland, St John's, NL, Canada
[2]Faculty of Sustainable Design Engineering, University of Prince Edward Island, Charlottetown, PE, Canada

***Abstract*—*This study investigates freezing dynamics of water droplets on coated steel substrates under controlled conditions. The freezing morphology and thermal evolution of droplets were analyzed using synchronized thermal and high-speed imaging techniques. The results provide insights into the relationship between coating properties, droplet characteristics, and freezing behavior, with potential applications in ice-prevention systems and thermal management solutions.*

***Keywords-component*—surface coatings; droplet impact; freezing**

I. INTRODUCTION

Detailed understanding of droplet impact on surfaces has advanced dramatically in recent decades, moving from simple observations to sophisticated quantitative analysis. When droplets collide with solid surfaces, they reveal complex fluid dynamics - particularly when freezing occurs. These insights have proven invaluable across industries, from optimizing inkjet printing technology to mitigating ice formation on ships and aircraft [1].

The understanding of droplet freezing during impact has advanced significantly through key studies. Hindmarsh et al. [2] established the fundamental role of convective heat transfer and thermal radiation in droplet freezing, demonstrating the importance of variable property models. Graeber et al. [3] showed that during impact, freezing initiates at the free surface and propagates inward while maintaining a liquid substrate interface, leading to self-dislodging behavior - a mechanism distinct from conventional impact-freezing models.

The dynamics of droplet impacts emerge from a complex interplay of forces, each dominating at different times and spatial scales. Inertial forces dominate initial deformation, followed by surface tension and viscous effects. To understand this complexity, researchers have identified two key parameters: the Weber number ($We = \frac{\rho V^2 d}{\sigma}$), which describes the droplet's spreading tendency, and the Ohnesorge number ($Oh = \frac{\mu}{\sqrt{\rho \sigma d}}$), which captures its resistance to flow. These parameters help predict whether a droplet will spread smoothly, splash dramatically, or perform anything in between [4].

Impact velocity fundamentally alters the impact regime. Low-velocity impacts result in spreading and recoil, whereas higher velocities trigger instabilities leading to splashing or breakup. Surface wettability influences contact line dynamics, while surface features modify local contact angles and energy dissipation mechanisms, altering global impact dynamics [5].

Once heat transfer is introduced, droplet impact acquires an additional layer of complexity. When the substrate is below the freezing point, the droplet may partially or fully solidify during the spreading or recoil stages [6]. This interplay between hydrodynamics and phase change is central to many real-world challenges, including marine icing, where the formation of ice on ships and offshore structures can lead to severe operational and safety hazards. The final frozen morphology—ranging from pointed protrusions to concave depressions—depends on the interplay of impact parameters, thermal conditions, and substrate properties [7].

Stone [8] presented ice-resistant design by focusing on droplet behavior rather than superhydrophobic methods, which fail under frost. The study proposed liquid-infused surfaces (SLIPS), examining ice hinges on droplet mobility before freezing, not just impact dynamics.

Recent experiments highlight the importance of droplet impact under freezing or supercooled conditions. Studies by Schremb *et al.* [9], Dehghani-Sanij *et al.* [10], and others have explored how variables like droplet and substrate temperatures, impact velocity, and fluid properties influence spreading and

freezing behaviors. Additionally, Eskin *et al.* [11] developed a model for freezing seawater droplets, considering salinity and temperature effects, which are pertinent to ice accretion on structures. They also highlight that the released latent heat from water solidification is crucial for the ice layer growth rate. Advanced models and machine learning approaches have further elucidated the governing factors, revealing the dominance of Weber and Reynolds numbers over temperature in certain conditions [4], [13], [14].

Collectively, these advances highlight the pivotal role of droplet impact in determining freezing onset, solidification patterns, and ultimately the macroscopic ice morphology. Ongoing efforts in marine icing prevention, for instance, must account for the intricacies of droplet impact dynamics and the associated heat transfer. Future developments will rely on high-fidelity experiments and robust numerical models to unravel the multiphysics nature of droplet impact and freezing, paving the way for more effective mitigation strategies for ice accretion on critical surfaces.

II. Experimental Setup

The experimental apparatus as shown in figure 1 was designed to investigate droplet impact dynamics and thermal behavior under controlled conditions. A droplet generator, consisting of a syringe mounted on a sturdy frame at a fixed height, was used to release droplets of varying volumes. Prior to impact, the droplets were precooled to 2°C to ensure uniform initial conditions. The droplets were then released from a height of 90 cm onto a steel substrate maintained at -15°C inside a freezer unit, simulating subzero marine environments. The study examined both uncoated steel and coated substrates with different thermal and surface properties. Surface characterization was performed using standard goniometric techniques to determine the wettability of each substrate.

Upon impact, the droplet underwent an initial spreading and recoiling phase due to inertial and surface tension effects, followed by rapid solidification as heat transferred to the cold substrate. The freezing process was characterized by the formation of an ice nucleation front, which propagated across the droplet until complete solidification. To capture the transient behavior and temperature evolution, a high-speed camera recorded the impact dynamics from above, while a thermal camera monitored heat dissipation and phase change progression.

In Equation (1), the Reynolds number is defined as:

$$Re = \frac{\rho D_0 v}{\mu} \tag{1}$$

where D_0 is the pre-impact droplet diameter, ρ is the fluid density, v is the impact velocity, and μ is the dynamic viscosity. This definition is used to characterize the relative importance of inertial and viscous forces during the droplet impact process.

Similarly, the Weber number (We) is defined as:

$$We = \frac{\rho v^2 d_0}{\sigma} \tag{2}$$

where ρ is the fluid density (999.8 kg/m^3), v is the impact velocity, d_0 is the pre-impact droplet diameter, and σ is the surface tension.

The impact velocities were determined experimentally using high-speed imaging through the following equation:

$$v = \frac{\Delta s}{\Delta t} = \frac{s_2 - s_1}{t_2 - t_1} \tag{3}$$

where: Δs is the distance traveled between two consecutive frames Δt is the time interval between frames ($\frac{1}{10000}$ s at 10,000 fps) s_2, s_1 are the droplet positions in consecutive frames t_2, t_1 are the corresponding time points.

The experiment uses a high-speed camera (Phantom V611) operating at 10,000 frames per second with high magnification zoom macro lens.

TABLE I presents the Reynolds and Weber numbers for different needle sizes at $h = 90$ cm.

TABLE. I
Reynolds and Weber Numbers for Different Needle Gauges at $h = 90$ cm

Droplet Diameter (mm)	Reynolds Number (Re)	Weber Number (We)
2.68	5,900	552
4.04	9,050	840
4.58	10,260	978

Larger droplets exhibit higher Re values, indicating greater inertial effects, while larger We values suggest a stronger tendency for droplet spreading upon impact due to reduced surface tension dominance. Detailed thermophysical and surface properties of the coatings and primers are summarized in Tables II and III.

TABLE. II
Physical characteristics and wettability of marine coating layers: measured coating thickness, surface roughness, and contact angles for different primers and marine coatings

Substrate	Thickness (mm)	Roughness (μm)	Contact Angles (°)	
			θ_A	θ_S
Primer A	0.0254	2.19	77.85	74.97
Primer B	0.2794	1.66	72.02	69.24
Coat A	0.5842	2.55	80.41	79.50
Coat B	0.3302	0.43	77.13	74.08
Coat C	0.1524	2.28	71.21	69.80

III. Results and Discussion

The spreading behavior over time was characterized by measuring the spread factor (D/D_0), defined as the ratio between spreading diameter (D) and initial droplet diameter (D_0). This dimensionless parameter was tracked for droplets impacting different coated surfaces as shown in figure 2. Specifically, droplets at an initial temperature (T_0) of 2 °C impacted surfaces maintained at -15 °C (T_s).

In the initial spreading phase, all surfaces exhibited nearly identical behavior, with the spread factor rapidly increasing

TABLE. III
THERMOPHYSICAL PROPERTIES OF COATINGS, PRIMERS, AND UNCOATED STEEL

Substrate	Density (kg/m^3)	Specific Heat (J/kgK)	Thermal Conductivity (W/mK)
Primer A	1170	1714	0.6662
Primer B	1115	739	0.7298
Coat A	1075	1534	0.5762
Coat B	1080	2255	0.3894
Coat C	1420	494	0.4712
Uncoated Steel	7850	490	45.000

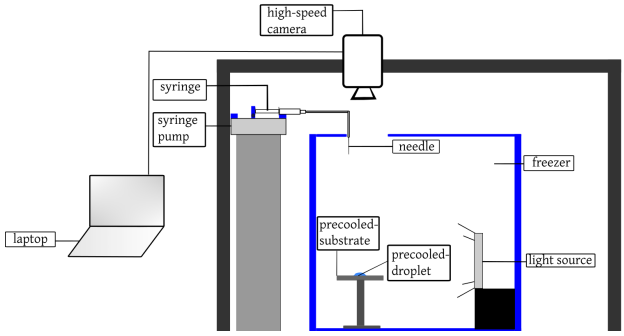

Figure. 1. Schematic representation of the experimental setup including the droplet generator, thermal camera, high-speed camera, and freezer.

to a maximum value of 3.5 within 3 seconds post-impact. Following this maximum spreading state, distinct differences emerged in the retraction and freezing dynamics across surface treatments. The uncoated steel substrate showed negligible retraction, maintaining a spread factor of 3.3 throughout the observation period, while primer-coated surfaces demonstrated intermediate behavior with Primer A and B stabilizing at spread factors of 2.9 and 2.7, respectively.

The marine coating systems (Coats A, B, and C) exhibited the most pronounced variations in retraction behavior. Coat A stabilized at an intermediate spread factor of 2.0, while Coats B and C displayed progressively enhanced retraction, reaching final spread factors of 1.6 and 1.4, respectively, at 30 seconds. This systematic variation in freezing morphology across different coating systems indicates that surface properties play a crucial role in determining the post-impact dynamics and final frozen configuration, with enhanced surface hydrophobicity promoting increased retraction before solidification.

The influence of initial droplet diameter (D_0) on spreading dynamics was investigated by comparing three different droplet sizes: 2.68, 4.04, and 4.58 mm and shown in figure 3. The evolution of the spread factor (D/D_0) reveals both similarities and distinct differences across these droplet sizes.

During the initial spreading phase (0-5 seconds), larger droplets achieved higher maximum spread factors, with the 4.58 mm droplet reaching approximately 3.9, compared to 3.7 for the 4.04 mm droplet and 3.5 for the 2.68 mm droplet. This trend suggests that increased droplet mass contributes to greater inertial spreading upon impact.

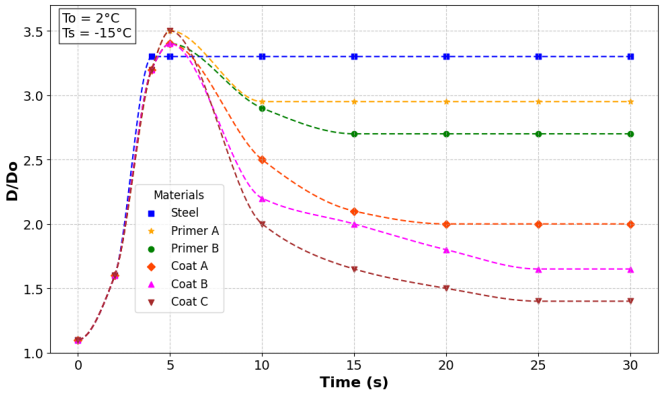

Figure. 2. Spread factor (D/D_0) dynamics for droplets impacting different surface coatings

The subsequent retraction phase showed size-dependent behavior. The smallest droplet (2.68 mm) exhibited the fastest retraction, reaching a stable spread factor of approximately 2.0 by 15 seconds. In contrast, the larger droplets (4.04 and 4.58 mm) demonstrated more gradual retraction, following similar trajectories until about 20 seconds, after which they stabilized at slightly different final spread factors of 1.8 and 1.9 respectively. The more prolonged retraction period for larger droplets suggests that increased mass delays the freezing process, allowing for extended contact line mobility before complete solidification.

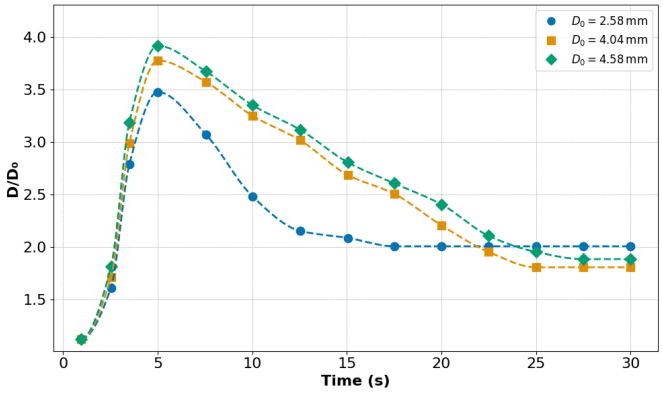

Figure. 3. Time variation of spread factor (D/D_0) for different initial droplet diameters showing size-dependent spreading and retraction behavior of Coat A.

The final frozen morphologies as illustrated in figure 4 reveal distinct patterns across different surface treatments. The uncoated steel surface exhibits a splat-like pattern with pronounced fingering at the periphery, indicating minimal retraction before freezing. Primer A and B show progressively more compact frozen shapes with smoother edges, suggesting increased retraction compared to the uncoated surface.

Marine coatings (Coat A, B, C) demonstrate the most significant influence on final morphology. These surfaces produce increasingly condensed droplet shapes, with Coat C showing the most pronounced retraction, resulting in a nearly spherical

cap formation. This progression in frozen morphology aligns with the spread factor measurements and correlates with the surface properties of each coating. The transition from spread-out patterns on steel to compact shapes on marine coatings illustrates how surface treatment fundamentally alters the competition between spreading, retraction, and solidification processes. The temperature profiles in figure 5 show characteristic stages of the freezing process and distinct thermal behaviors across surface treatments. The uncoated steel surface demonstrates the most rapid thermal response, with complete freezing occurring within approximately 5 seconds. This rapid freezing corresponds to its high thermal conductivity and efficient heat transfer properties.

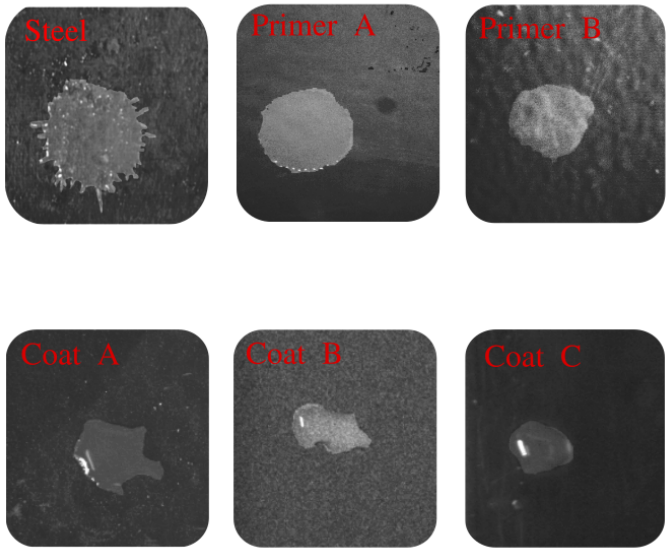

Figure. 4. Final frozen morphology of droplets on different surface treatments: uncoated steel, primer coatings (Primer A, B), and marine coatings (Coat A, B, C).

Primer coatings exhibit intermediate freezing durations, with Primer A and B showing complete solidification in 8 and 10 seconds respectively. A notable feature in these profiles is the presence of a recalescence peak (sharp temperature rise) followed by a more gradual cooling phase, indicating the release of latent heat during nucleation and subsequent freezing.

Marine coatings demonstrate significantly extended freezing times, with Coat A requiring about 17 seconds, Coat B approximately 20 seconds, and Coat C showing the longest freezing duration of around 30 seconds. These coatings display distinct plateau regions in their temperature profiles, suggesting prolonged phase transition periods. The extended freezing times correlate with the coatings' lower thermal conductivity, which reduces heat transfer rates between the droplet and the substrate.

The systematic increase in freezing duration from uncoated steel to marine coatings aligns with the previously observed spreading dynamics and final morphologies, demonstrating how surface thermal properties fundamentally influence the freezing process.

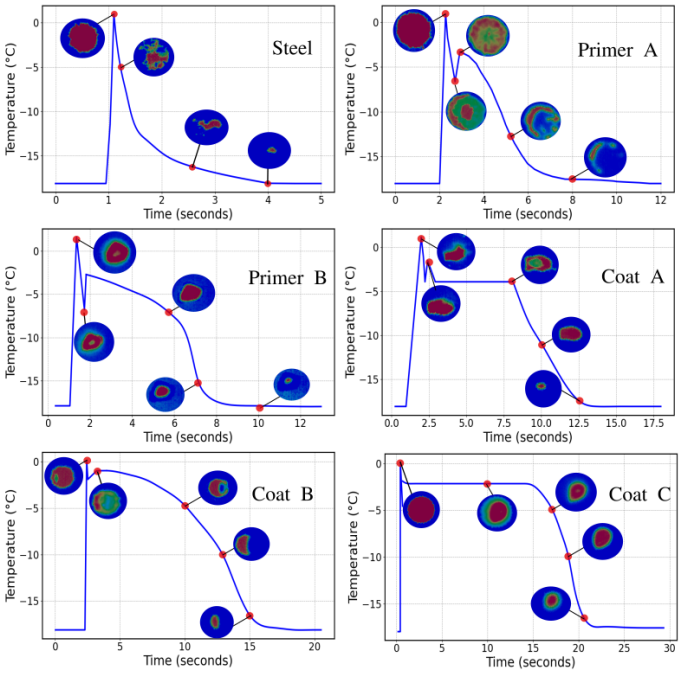

Figure. 5. Substrate temperature evolution at the impact point for different surface treatments.

The final frozen morphologies (Fig. 4) indicate that uncoated steel undergoes minimal retraction, while surfaces with marine coatings exhibit greater droplet mobility before solidification. This behavior corresponds closely to the substrate temperature profiles (Fig. 5), where lower thermal conductivity coatings prolong freezing times and allow for more pronounced retraction. Taken together, these observations underscore how surface properties govern both droplet dynamics and thermal transport during freezing.

IV. Conclusion

This study investigated the impact and freezing behavior of supercooled water droplets on various coated steel substrates under subzero conditions. By systematically varying the droplet size, substrate temperature, and coating properties, we demonstrated that reduced thermal conductivity and enhanced surface hydrophobicity promote retraction before solidification, resulting in more compact frozen morphologies. In contrast, uncoated steel substrates with high thermal conductivity experienced rapid freezing and minimal droplet retraction. These findings highlight the critical influence of substrate thermal properties and wettability on ice formation, providing insights that can inform the engineering of anti-icing solutions in marine, aerospace, and energy sectors.

Future works could focus on investigating oblique (angled) droplet collisions, which may reveal additional complexities in spreading, splashing thresholds, and freezing mechanisms. Further, the testing of novel superhydrophobic or ice-phobic

materials would broaden our understanding of how different surface chemistries mitigate icing under harsh conditions. Incorporating high-speed imaging with computational fluid dynamics (CFD) simulations could offer detailed spatiotemporal insights into heat transfer and phase-change processes. Additionally, studying droplets containing dissolved salts or other impurities would help extend our findings to real-world marine and cold-region scenarios, where contamination effects are often significant. By pursuing these directions, future research can refine strategies for droplet freezing control, ultimately leading to more efficient anti-icing and de-icing technologies.

ACKNOWLEDGMENT

Financial support from the Natural Sciences and Engineering Research Council of Canada (NSERC) is gratefully acknowledged.

REFERENCES

[1] Wang, X., Xu, B., Guo, S., Zhao, Y., Chen, Z. (2023). Droplet impacting dynamics: Recent progress and future aspects." *Advances in Colloid and Interface Science*, 317, 102919.

[2] Hindmarsh, J.P., Russell, A.B., Chen, X.D. (2003). Experimental and numerical analysis of the temperature transition of a suspended freezing water droplet. *International Journal of Heat and Mass Transfer*, 46, 1199-1213.

[3] Graeber, G., Schutzius, T.M., Eghlidi, H., Poulikakos, D. (2017). Spontaneous self-dislodging of freezing water droplets and the role of wettability. *Proceedings of the National Academy of Sciences*, 114(42), 11040-11045.

[4] Lam, L.S., Sultana, K.R., Pope, K., Muzychka, Y.S. (2020). Effect of thermal transport on solidification of salt and freshwater water droplets on marine surfaces." *International Journal of Heat and Mass Transfer*, 153, 119452.

[5] Jung, Y.C., Bhushan, B. (2008). Dynamic Effects of Bouncing Water Droplets on Superhydrophobic Surfaces." *Langmuir*, 24(12), 6262-6269.

[6] Naterer, G.F. (2011). "Multiphase transport processes of droplet impact and ice accretion on surfaces." *Cold Regions Science and Technology*, 65(1), 5-12.

[7] Mishchenko, L., Hatton, B., Bahadur, V., Taylor, J.A., Krupenkin, T., Aizenberg, J. (2010). Design of Ice-free Nanostructured Surfaces Based on Repulsion of Impacting Water Droplets." *ACS Nano*, 4(12), 7699-7707.

[8] Stone, H.A. (2012). Ice-Phobic Surfaces That Are Wet. *ACS Nano*, 6(8), 6536-6540.

[9] Schremb, M., Roisman, I. V., Tropea, C. (2018). "Normal impact of supercooled water drops onto a smooth ice surface: experiments and modelling." *Journal of Fluid Mechanics*, 835, 1087-1107.

[10] Dehghani-Sanij, A.R., MacLachlan, S., Naterer, G.F., Muzychka, Y.S., Haynes, R.D., Enjilela, V. (2020). "Multistage cooling and freezing of a saline spherical water droplet." *International Journal of Thermal Sciences*, 147, 106095.

[11] Eskin, D., Fisher, G., Vulf, M., Chugunov, S., & Johansen, S. T. (2024). Simulation of freezing a sea water droplet moving in a cold air. *Cold Regions Science and Technology*, 223, 104226.

[12] Kant, P., Koldeweij, R.B.J., Harth, K., van Limbeek, M.A.J., Lohse, D. (2020). "Fast-freezing kinetics inside a droplet impacting on a cold surface." *Proceedings of the National Academy of Sciences*, 117(6), 2788-2794.

[13] Keshavarzi, S., Sourati, J., Momen, G., Jafari, R. (2022). Temperature-dependent droplet impact dynamics of a water droplet on hydrophobic and superhydrophobic surfaces: An experimental and predictive machine learning-based study. *International Journal of Heat and Mass Transfer*, 195, 123190.

[14] Puolakka, O. (2024). "Droplet supercooling in marine icing tests." *Cold Regions Science and Technology*, 219, 104121.